ACS APPLIED BIO MATERIALS

Open Access

This article is licensed under CC-BY 4.0

www.acsabm.org

Article

Cytotoxicity Investigation of $Ti_3C_2T_x$ MXene toward Human Umbilical Vein Endothelial Cells

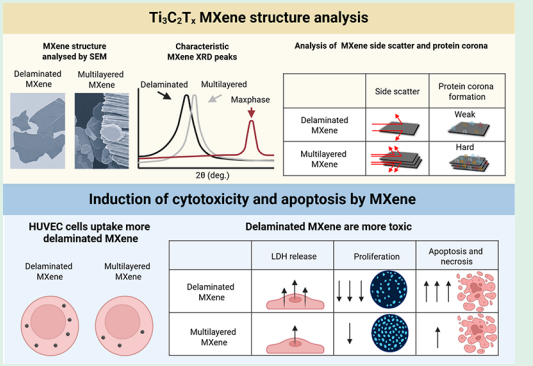
Rokas Miksiunas,* Rusne Uzielaite, Simonas Ramanavicius, Sonata Adomaviciute-Grabusove, Sigita Bendinskaite, Kieran Brennan, Alfonso Blanco, Maksym Pogorielov, Viktoriia Korniienko, Daiva Bironaite, Oleksiy Gogotsi, and Arunas Ramanavicius*

Cite This: *ACS Appl. Bio Mater.* 2026, 9, 8158–8168

Read Online

ACCESS | Metrics & More | Article Recommendations | Supporting Information

ABSTRACT: MXenes are emerging two-dimensional nanomaterials with promising potential for biomedical applications, including osteogenic differentiation, antibacterial properties, anticancer therapy, and drug delivery systems. However, biocompatibility studies with blood vessels or endothelial cells need more thorough research. In this study, delaminated and multilayered $Ti_3C_2Ti_x$ MXenes were synthesized from the Ti_3AlC_2 MAX phase and characterized by scanning electron microscopy (SEM) and X-ray diffraction (XRD) and applying violet, blue, and red side scatter width (SSC-Width) and high (SSC-H) functions of a flow cytometer. MXene-cell association was examined using the red side scatter area (SSC-A) function of the flow cytometer. HUVEC responses following 1- and 3-day exposure to MXenes were evaluated by nuclei count and LDH release. Apoptosis was also evaluated with a flow cytometer and Annexin V/propidium iodide staining. Both types of MXene were associated with HUVECs and showed a concentration-dependent response; however, delaminated 2D-like MXene flakes were significantly more cytotoxic than multilayered 3D-like MXenes: at low concentrations (1–3 μg/mL), their cell number started decreasing, LDH release increased, and late apoptosis and necrosis were induced, while multilayered MXenes showed similar effects at a much higher concentration, at 25 μg/mL. Comparing the influence of two different structures of MXenes suggests that the delaminated MXenes may exhibit enhanced MXene-cell interactions than multilayered MXenes, which is leading to membrane perturbation and subsequent effects on cell viability and apoptosis. Overall, these findings demonstrate that advanced, multiparametric, and high-performance flow cytometry can be used not only for the cell analysis but also for the identification of nanoparticle size, and MXene-cell association. Data also shows that biocompatibility of delaminated and multilayered $Ti_3C_2Ti_x$ MXene in HUVECs is a strongly preparation-dependent process, which highlights the importance of evaluation of standardized biocompatibility strategies for the development of safe MXene-based biomedical applications.



KEYWORDS: *MXene, endothelial cells, flow cytometry, cytotoxicity, apoptosis, SEM*

1. INTRODUCTION

Two-dimensional (2D) materials have attracted significant attention due to their unique physiochemical properties, including high surface area, tuneable surface chemistry, and favorable electrochemical characteristics.[1] Among these, MXene—a family of transition metal carbides and nitrides with formula $Ti_3C_2T_x$, have emerged as promising candidates for physical, chemical, and biomedical applications.[2] The general formula of MXenes is $M_{n+1}X_nT_x$ (n = 1–3), where M is an early transition metal, X is carbon and/or nitrogen, and T_x represents surface functional groups (e.g., –OH, –O, –F, Cl, or S).[3] 2D carbides, nitrides, or carbonitrides are produced by selectively etching group IIIA–VA elements (e.g., Al, Sn, and Si) from MAX phase precursors, enabled by the greater acid reactivity of M–A metallic bonds than M–X covalent or ionic bonds.[4] Based on the synthesis route and etching process, it is possible to synthesize several types of MXene from the Ti_3AlC_2 MAX phase: Delaminated MXene are synthesized using lithium fluoride (LiF) and lithium chloride (LiCl) to generate single-layered flakes, while multilayered MXenes are etched only with hydrogen fluoride (HF) by removing aluminum (Al) layers but making structure still intact.[5] Both types of MXene are used for quite similar applications, which include energy storage and

Received: May 18, 2026
Revised: July 23, 2026
Accepted: July 24, 2026
Published: August 12, 2026



Downloaded from pubs.acs.org/aabmcb/article-pdf/9/17/8158/6651707/mt-2026-01000s.pdf by VILNIUS UNIV user on 04 November 2026

© 2026 The Authors. Published by American Chemical Society

https://doi.org/10.1021/acsabm.6c01000
ACS Appl. Bio Mater. 2026, 9, 8158–8168

water purification; however, single-layered MXenes are better catalyst components in flexible wearable electronics or sensors than multilayered MXenes.[6,7] In terms of biological applications, multilayered MXenes have been shown to promote osteogenic differentiation, while delaminated MXenes are currently investigated for their antibacterial properties, anticancer therapy, and drug delivery systems.[8−10]

Despite increasing interest in MXene-based biomedical platforms, their biocompatibility remains incompletely understood. The biological response to MXene varies depending on cell type, exposure conditions, and MXene preparation methods. The MXene etching processes use HF, LiF, LiCl, and other etchants, which could remain in the structure despite additional washing steps and affect cell viability. Moreover, there is evidence that MXene can produce reactive oxygen species (ROS), which may trigger apoptosis and cell death,[8] while other data indicate that MXene can be biocompatible without generating ROS.[10] In addition, some studies emphasize cellular membrane disruption as the main mechanism,[9] revealing MXene acting as a "nano-knife" and a mechanically damaging cell membrane.[11−13] It was also shown that under electric current, MXene flakes could move inside cells and directly damage DNA identified by the comet assay.[14] Likely, these mechanisms mostly depend on MXene synthesis route, etchant, and MAX phase materials from which 2D MXene sheets are synthesized. However, direct interaction between membrane phospholipids and MXene *via* ionic interaction, hydrophobic and van der Waals forces, and membrane destabilization leading to the cell integrity destabilization can also occur.[15]

Direct contact between nanomaterials and cell membrane is usually induced by endocytosis, pinocytosis, phagocytosis, or direct entry *via* spontaneous membrane penetration.[16,17] Previous research illustrates that cells can uptake up to 500 nm size spherical particles that are not mechanically damaging cell membranes.[18] 2D nanomaterials, such as graphene oxide or molybdenum disulfide (MoS_2), are thin enough to be internalized in the cells by up to 10 μm sheets in lateral dimensions.[17] Previous MXene studies showed that transmission electron microscopy (TEM) can be used to identify MXene in the cells.[19,20] However, the biocompatibility and uptake of MXene and HUVEC with other, more exact and quick methods, such as flow cytometry, have not been investigated.

In this study, we were aiming to investigate the biocompatibility and MXene–cell association at various concentrations of delaminated and multilayered MXene during 1 and 3 days of optimal HUVEC growth conditions. MXene–cell association, cell viability, and apoptosis induction by MXene in HUVECs were evaluated using flow cytometry (Figure 1). By integrating structural MXene characterization with cellular viability and apoptosis induction assays using flow cytometry, this work aims to clarify how different types of MXene, such as delaminated and multilayered, affect HUVEC cells for the further development of safe biomedical implementations.

2. RESULTS AND DISCUSSION

2.1. Characterization of Delaminated and Multilayered MXenes with Scanning Electron Microscopy (SEM) and X-ray Powder Diffraction (XRD)

The SEM micrographs show that the Ti_3AlC_2 MAX phase (Figure 2a) exhibits a highly multilayered and irregular structure, whereas multilayered MXenes display a more organized, 3D-like morphology with lateral dimensions of approximately 2–4 μm (Figure 2b). In contrast, delaminated MXenes appear as thin, 2D flake-like structures, with a thickness of approximately 1–2 nm and larger lateral dimensions of about 5–10 μm (Figure 2c). In addition, the phase composition of the materials was analyzed by X-ray diffraction (XRD). As shown in Figure 2d, the shift of the (002) peak from ∼10 to ∼7° indicates the transition from the MAX phase to MXene.[21] In the 35–80° range, multilayered MXenes still exhibit small residual peaks corresponding to the MAX phase, indicating incomplete etching of interlayers between MXene loayers.[9,22] The multilayered MXene displays sharper and more intense peaks (second pattern), suggesting higher crystallinity and the presence of more well-defined crystal planes or possibly the presence of multiple phases. In contrast, broader and weaker peaks (third pattern) indicate lower crystallinity, a simpler structure, or fewer detectable planes. XRD-based analysis further suggests that multilayered MXenes have a higher degree of atomic ordering within specific crystal planes, which is associated with larger crystalline domains and their stacked, multilayered structure.

2.2. Protein Corona Formation Analysis on MXenes by ATR-FTIR

In parallel with SEM and XRD analyses, delaminated and multilayered MXene were investigated for protein corona formation using attenuated total reflectance Fourier transform infrared spectroscopy (ATR-FTIR). When MXene nanoparticles enter biological fluids, proteins and other biomolecules can adsorb onto their surfaces, forming a protein corona that may alter cellular uptake, biodistribution, and cytotoxicity.[23] HUVEC cells are typically cultured with large vessel endothelial supplement (LVES), which contains 2% of fetal bovine serum (FBS), whereas many other authors culture cells in media supplemented with 10% of serum.

Our results showed that the most extensive protein corona on both delaminated and multilayered MXenes was formed after 3 days of incubation in HUVEC medium containing 10% of FBS, as indicated by the ATR-FTIR spectra (Figure 3a,b). The main ATR-FTIR peaks associated with proteins are the amide I and amide II bands, which correspond to protein secondary structures as well as N–H bending and C–N stretching vibrations (Figure 3a,b).[24]

In contrast, protein corona formation in HUVEC medium containing LVES was observed only on multilayered MXene. Specifically, the characteristic spectral change associated with the amide I band at approximately 1643 cm^{-1} was not observed for delaminated MXene, suggesting the absence of a detectable protein corona or substantially lower protein adsorption under these conditions (Figure 3a,b).

Protein corona formation can modulate nanoparticle–cell interactions and, in some cases, reduce nanoparticle uptake.[25] Therefore, the lack of a detectable protein corona on delaminated MXenes in the HUVEC culture medium with LVES may contribute to its higher cytotoxicity toward HUVECs compared with multilayered MXenes.

2.3. Characterization of Delaminated and Multilayered MXenes by Flow Cytometry

In parallel with SEM, XRD, ATR-FTIR analyses, light scattering was assessed using a CytoFLEX XL flow cytometer and

Downloaded from pubs.acs.org/aabmcb/article-pdf/9/17/8158/6651507/mt-2026-01000s.pdf by VILNIUS UNIV user on 04 November 2026

https://doi.org/10.1021/acsabm.6c01000
ACS Appl. Bio Mater. 2026, 9, 8158−8168

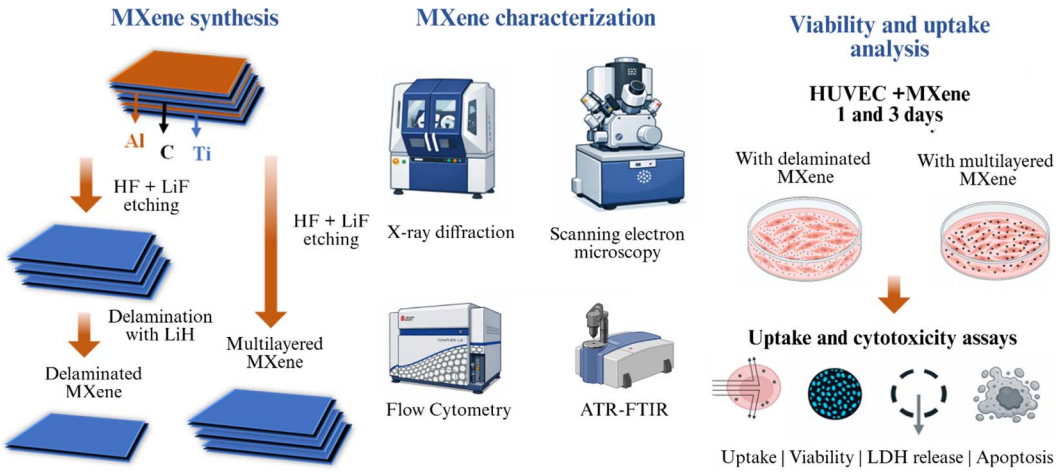


Figure 1. Experimental scheme of delaminated and multilayered MXene synthesis and characterization, HUVEC viability, and MXene uptake analysis with flow cytometry. Scheme was made using Biorender software.

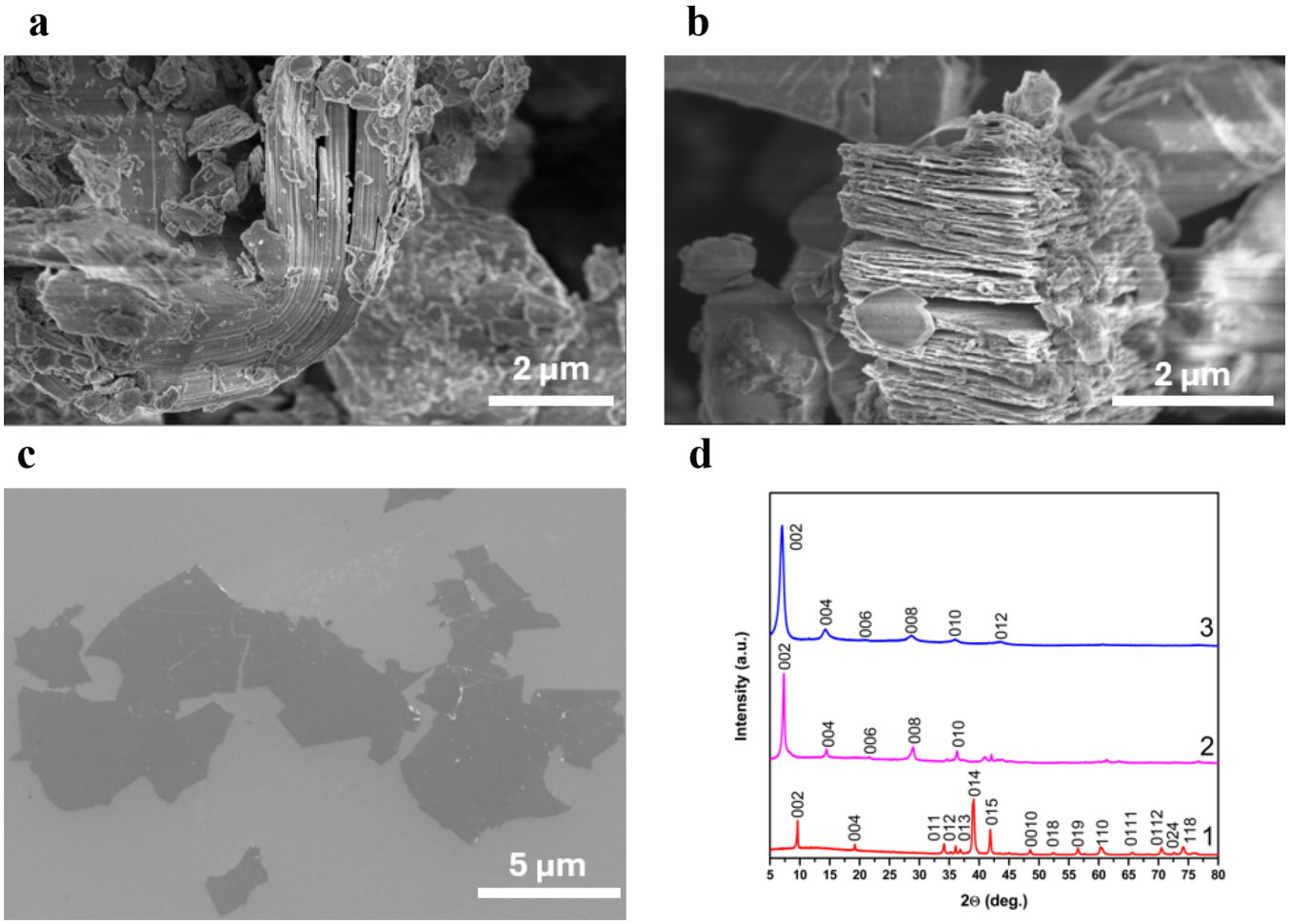


Figure 2. Surface analysis of MAX phase, multilayered, and delaminated MXene by SEM and XRD. (a) Scanning electron microscopy (SEM) image of the $Ti_3C_2T_x$ MAX phase. (b) SEM image of multilayered $Ti_3C_2T_x$ MXene. (c) SEM image of single-layered (delaminated) $Ti_3C_2T_x$ MXene. (d) X-ray powder diffractometer (XRD) patterns of the first line—$Ti_3C_2T_x$ MAX phase, second line—multilayered $Ti_3C_2T_x$ MXene, and third line—single-layered (delaminated) $Ti_3C_2T_x$ MXene.

Downloaded from pubs.acs.org/aabmcb/article-pdf/9/17/8158/6651507/mt-2026-01000s.pdf by VILNIUS UNIV user on 04 November 2026

https://doi.org/10.1021/acsabm.6c01000
ACS Appl. Bio Mater. 2026, 9, 8158−8168

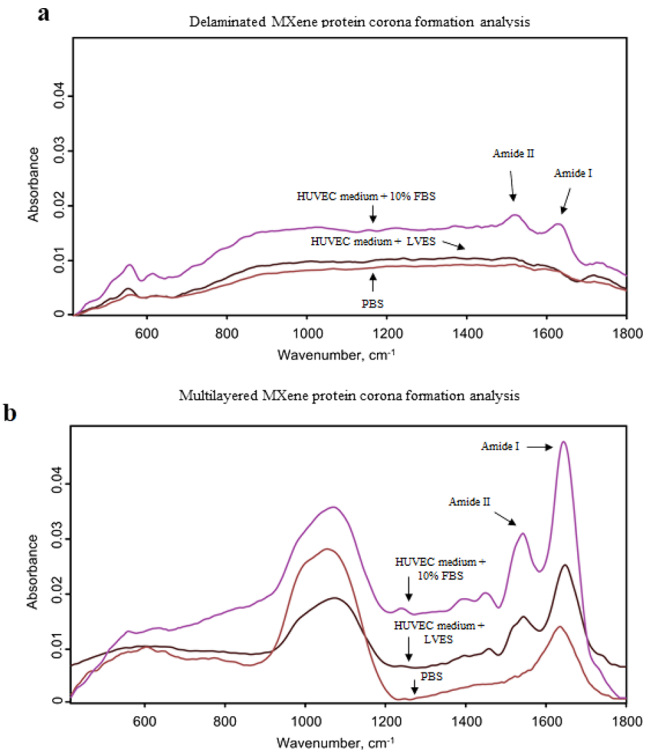


Figure 3. Protein corona formation analysis on delaminated and multilayered MXene with attenuated total reflectance Fourier-transform infrared spectroscopy. ATR-FTIR analysis of delaminated (a) or multilayered (b) MXene after 72 h of incubation in HUVEC medium with LVES supplement, HUVEC medium with 10% of FBS and PBS.

compared with the corresponding SEM and XRD data. Analysis with the red and violet laser using the height parameter (SSC-Height) revealed that multilayered MXenes compared to delaminated MXenes displayed a population shifted toward higher violet and red side-scatter intensities, indicating differences in their optical scattering properties (Figure 4a,b). This is likely because delaminated MXenes are smaller in size (2–4 μm in lateral dimension) and consist of single-layered 2D structures, whereas multilayered MXenes are larger (5–10 μm in lateral dimension) and exhibit a more complex, 3D-like stacked morphology (Figure 4a,b).

Delaminated MXenes, being thin and flexible 2D sheets, are more prone to random orientation and bending compared to multilayered MXene-based structures. This results in longer signal duration as they pass through the laser beam, leading to higher side scatter width (SSC-width) values.[26]

Analysis using the side scatter height (SSC-H) parameter with violet, blue, and red lasers showed that multilayered MXene scattered light several orders of magnitude more intensely than delaminated MXene (Figure 4b). This is likely due to their stacked, multilayered structure, which enhances light scattering compared to the thinner, delaminated sheets. Multilayered MXenes also exhibited significantly higher scattering of violet and red light compared to blue light scattering. This suggests that their more complex structure of multilayered MXene enhances scattering, particularly at shorter (violet) and longer (red) wavelengths, while blue light is scattered less intensively in comparison to violet and red light. Consistent with this, other studies have shown that larger particles exhibit higher SSC-width signals, which depend on parameters such as particle size and refractive index.[27−29]

Overall, these measurements demonstrate that flow cytometry can be effectively used to compare MXene light-scattering patterns.

2.4. Flow Cytometric Analysis of MXene-HUVECs Association

After analyzing the light-scattering characteristics of both MXenes with flow cytometry, their uptake by HUVEC cells was also evaluated. Association was assessed using the red laser side scatter area (SSC-A) parameter after 1 and 3 days of exposure to MXene. The red SSC-A signal is commonly used to estimate particle uptake, as the red laser penetrates cells more effectively than violet or blue lasers.[30]

Both delaminated and multilayered MXene preparations were internalized by HUVEC cells after 1 and 3 days of incubation (Figure 5a,b, respectively). However, HUVEC cells more readily associated with delaminated MXenes (1–25 μg/mL) compared to multilayered ones. Furthermore, after 3 days of incubation, association of delaminated MXenes at 25 μg/mL appeared to reach saturation, whereas uptake of multilayered MXene continued to increase.

These results suggest earlier SSC-A signal saturation for delaminated MXene. Consistent with this observation, previous studies have shown that cells can internalize thin graphene flakes with lateral dimensions of up to 10 μm, similar to the delaminated MXene used in this study.[17]

2.5. Nuclei Count and LDH Release after the Incubation of HUVEC Cells with Delaminated and Multilayered MXenes

Different concentrations of delaminated and multilayered MXenes were applied to HUVEC cells, and nuclei count and LDH release were evaluated after 1 and 3 days of incubation.

Both cell viability assays showed that delaminated MXenes were more cytotoxic than multilayered ones (Figure 6). Nucleic count analysis demonstrated that, after 1 day of incubation, 3 μg/mL of delaminated MXenes began to reduce the cell number, while after 3 days, even 1 μg/mL already exhibited cytotoxic effects (Figure 6). In contrast, multilayered MXenes required a concentration of 25 μg/mL to affect cell viability over the same incubation periods (Figure 6c).

The LDH release assay showed that 3 μg/mL of delaminated MXenes induced LDH release after 1 day of incubation, whereas a higher concentration (25 μg/mL) resulted in significant LDH release only after 3 days of incubation (Figure 6c). In contrast, multilayered MXenes at 25 μg/mL caused only a slight increase in LDH release after 1 day, and no significant cytotoxic effect was observed 3 days later compared to that registered in the control sample (Figure 6d). Overall, both assays indicated that the effect of delaminated-MXene-containing sample was stronger than that induced by multilayered MXenes. The discrepancy between the effects observed in nuclei count and LDH release assays may be explained by the sensitivity of HUVEC cells to growth conditions. After 3 days of incubation, cells likely reached confluence, which may have a stronger effect on LDH release than on nucleic count.

Previous studies have shown that delaminated MXenes typically exhibit cytotoxic effects after 24 h at concentrations of 25 μg/mL or higher.[20,31] MXene cytotoxicity is influenced by multiple factors, including cell type and culture conditions, MXene dose, composition and synthesis, surface

Downloaded from pubs.acs.org/aabmcb/article-pdf/9/17/8158/6651507/mt-2026-01000s.pdf by VILNIUS UNIV user on 04 November 2026

https://doi.org/10.1021/acsabm.6c01000
ACS Appl. Bio Mater. 2026, 9, 8158−8168

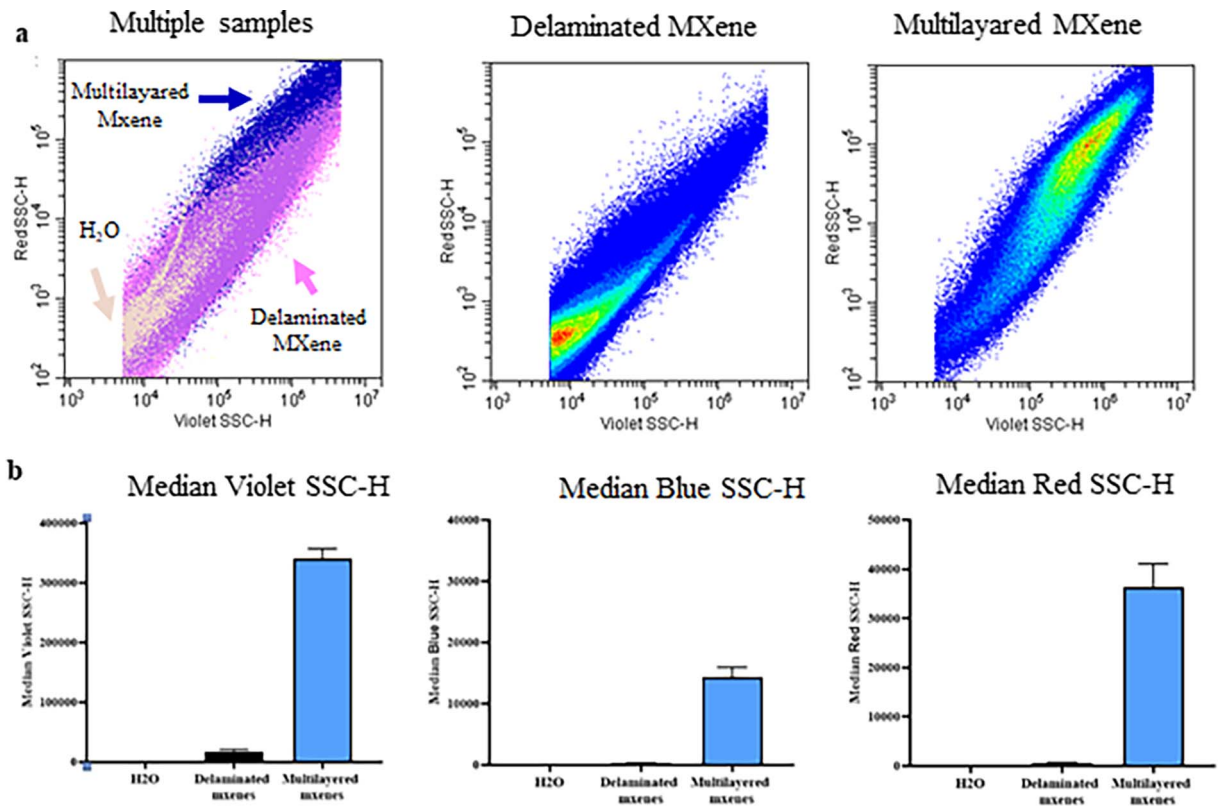


Figure 4. Flow cytometry analysis of delaminated and multilayered MXene. (a) Flow cytometry based assessment of MXene containing sample analyzed by side scatter width (SSC-Height). (b) Median fluorescence intensity (MFI) of MXene analyzed with violet, blue, and RED SSC-H.

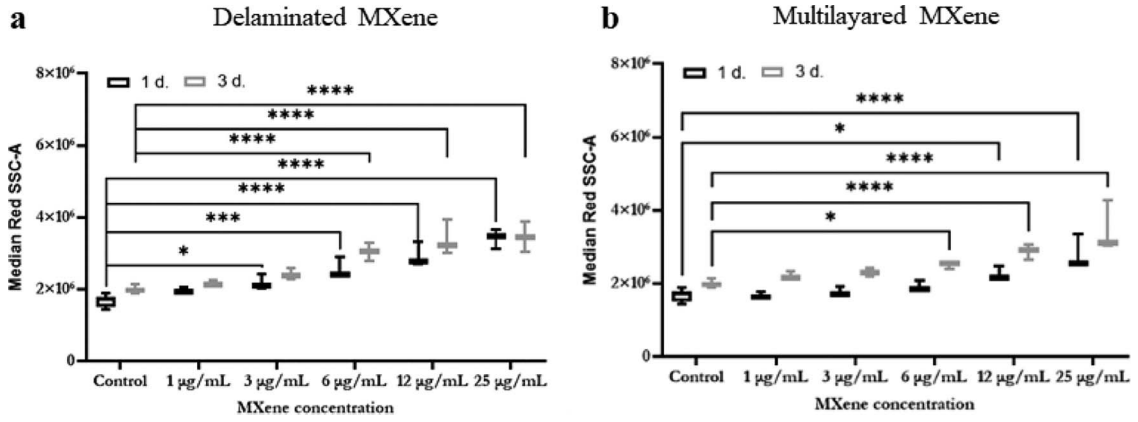


Figure 5. Flow cytometry analysis of MXene-HUVEC association after 1 and 3 days of incubation. (a) RED SSC-A of HUVEC with delaminated MXenes. (b) RED SSC-A of HUVEC with multilayered MXenes. Statistical analysis was done with two-way ANOVA. Data are statistically significant at $*p \leq 0.05$, $***p \leq 0.001$, and $****p \leq 0.0001$ levels, $n = 6$, from three experiments comparing HUVEC cells without and with MXenes.

modifications, particle size, and exposure duration.[32−34] In the present study, HUVEC cells were cultured in HUVEC medium containing 2% of LVES, whereas in other studies, HUVECs exposed to MXenes were cultured in DMEM containing 10% of FBS.[35−37] Studies with silica nanoparticles have demonstrated that serum proteins can adsorb onto nanoparticle surfaces, forming a protein corona that reduces cellular uptake and, consequently, the cytotoxicity of silica nanoparticles.[38]

Therefore, MXenes in HUVEC medium containing only 2% of LVES are likely less coated by serum proteins, which may facilitate their uptake within HUVEC cells and contribute to the increased cytotoxicity of MXenes, which was observed in this study.

2.6. Evaluation of Apoptosis after the Incubation of HUVEC Cells with Delaminated and Multilayered MXenes

Cell count decrease and LDH release assays demonstrated cytotoxic effects of MXenes on cell viability; however, their effects on the induction of apoptosis remain unclear. Therefore, early

Downloaded from pubs.acs.org/aabmcb/article-pdf/9/17/8158/6651707/mt-2026-01000s.pdf by VILNIUS UNIV user on 04 November 2026

https://doi.org/10.1021/acsabm.6c01000
ACS Appl. Bio Mater. 2026, 9, 8158−8168

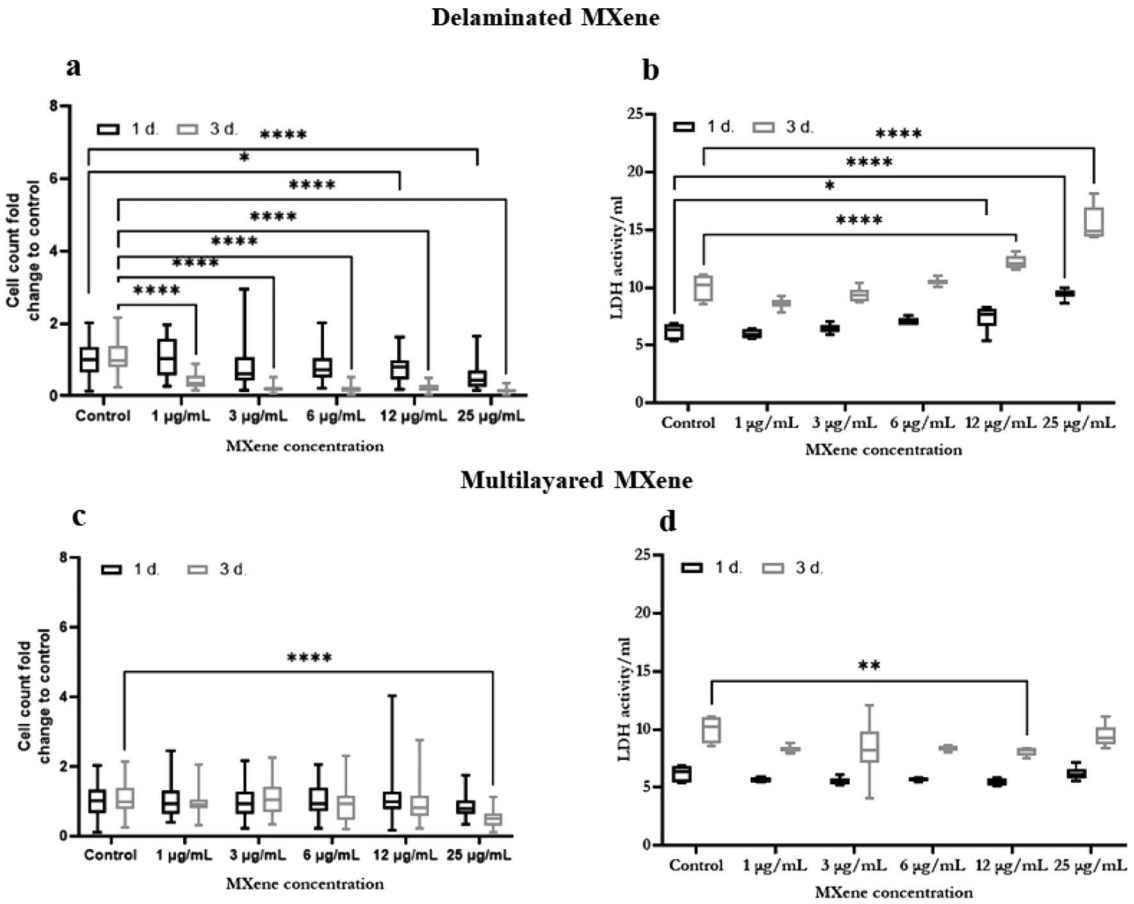


Figure 6. HUVEC cell number and LDH release assays investigating effects of delaminated and multilayered MXene after 1 and 3 days of exposure. HUVEC cell number (a) and LDH release (b) after exposure to different concentrations of delaminated MXenes for 1 and 3 days. HUVEC cell number (c) and LDH release (d) after 1 and 3 days of exposure to different concentrations of multilayered MXenes. Data are shown as mean ± standard deviation (SD). The data are significant at $*p \leq 0.05$, $**p \leq 0.01$, and $****p \leq 0.0001$, $n = 6$, from three experiments comparing HUVEC cells without and with MXene. Two-way ANOVA was calculated by the GraphPad Prism 9 program.

apoptosis, late apoptosis, and necrosis were evaluated by flow cytometry using an Annexin V/PI assay.

Cell viability results were confirmed by the apoptosis assay, which confirmed that delaminated MXenes induced stronger effects than multilayered MXenes, particularly in promoting late apoptosis and necrosis (Figures 7 and 8). Delaminated MXenes, at concentrations of 1–3 μg/mL, began to induce late apoptosis, reaching a maximum of approximately 20% at 25 μg/mL after 1 and 3 days of exposure (Figure 7b). In contrast, multilayered MXenes induced only about 4% late apoptosis at 25 μg/mL, with a more pronounced effect observed after 1 day than 3 days of incubation (Figure 8b).

Delaminated MXenes, within a similar concentration range (1–3 μg/mL), also started to induce necrosis, reaching a maximum of approximately 10% at a concentration of 6 μg/mL (Figure 7c), whereas multilayered MXenes at 25 μg/mL induced only around 2% of necrosis (Figure 8c). Notably, at 25 μg/mL, the effects of delaminated MXenes reached saturation on induction late apoptosis and necrosis, whereas multilayered MXenes showed weaker effects.

At 25 μg/mL, the effects of delaminated MXenes appeared to plateau, whereas multilayered MXenes showed weaker effects. Several studies suggest that MXene toxicity is associated with either generation of ROS or direct interaction with the cell membrane.[39,40] The single-layered MXene used in this study, with a thickness of 1–2 nm and lateral dimensions of 5–10 μm, therefore, they potentially may act according to "nano-knife" mechanism, which has been proposed for bacterial cells, physically damaging cellular structures, including the cell membrane and potentially even DNA.[41,42] The "nano-knife" mechanism has already been demonstrated in several publications involving bacteria where it was shown to disrupt the bacterial cell wall.[12,13] Eventually, the "nano-knife" mechanism may explain why delaminated MXenes exhibit greater cytotoxicity than multilayered forms. In addition, the data from this study showed that ROS generation is not the cause of HUVEC cytotoxicity, because no ROS generation was observed in HUVEC cells after exposure to 25 μg/mL of either delaminated or multilayered MXene for 2, 4, or 24 h (Figure S1).

Thus, advanced, multiparametric, and high-performance flow cytometry study of delaminated and multilayered MXene light scattering, cell association, and cytotoxicity revealed the delaminated MXene having a larger surface area and lower detectable protein adsorption, being sharper with thinner 2D edges, having higher dispersibility and cellular contact than the multilayered MXene, therefore having greater MXene-cell association accompanied by stronger cytotoxicity

Downloaded from pubs.acs.org/aabmcb/article-pdf/9/17/8158/6651707/mt-2026-01000s.pdf by VILNIUS UNIV user on 04 November 2026

https://doi.org/10.1021/acsabm.6c01000
ACS Appl. Bio Mater. 2026, 9, 8158–8168

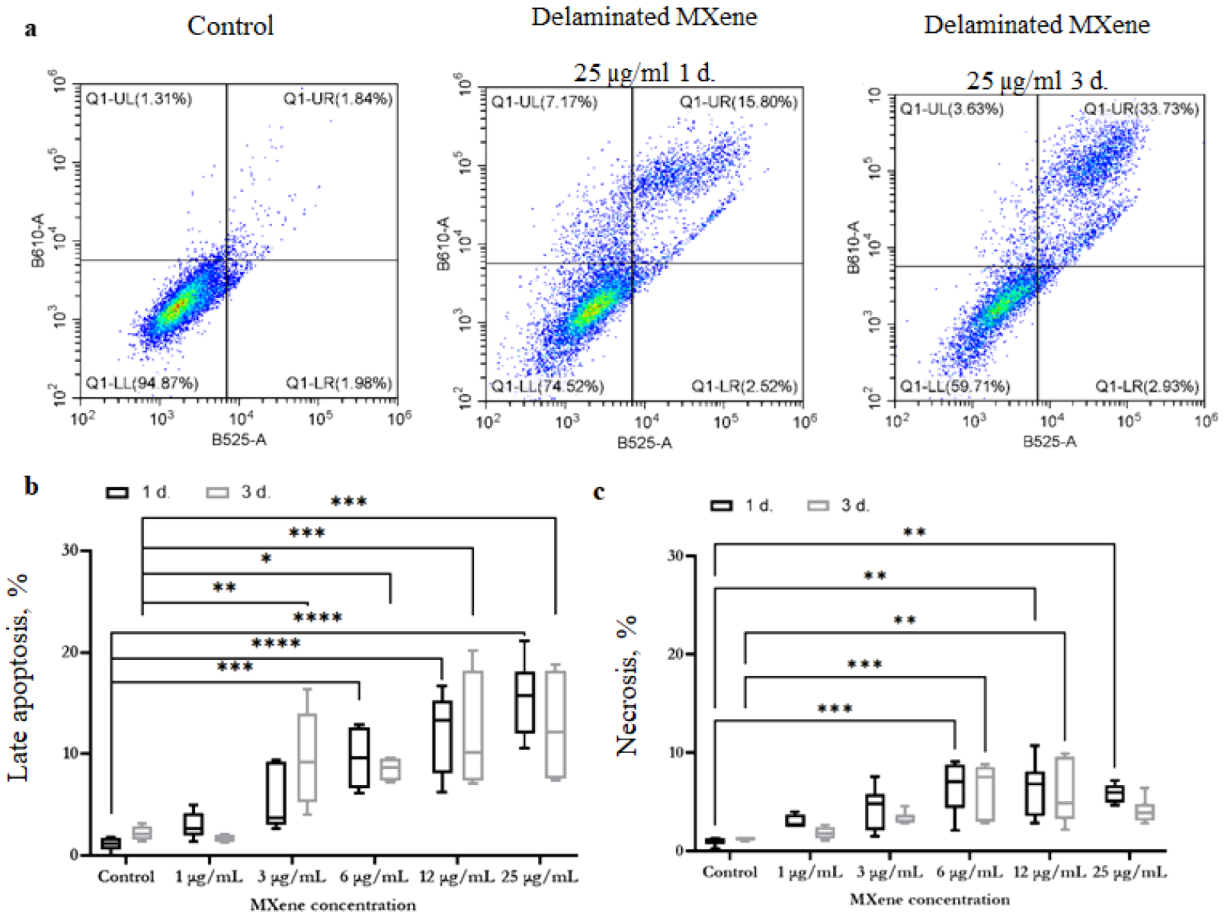


Figure 7. The assessment of late apoptosis (Annexin V with PI) and necrosis (PI) in HUVEC cells after 3 days of exposure to delaminated MXene. (a) HUVEC cells flow charts—control cells, cells with 25 μg/mL delaminated MXene after 1 day and 3 days of exposure. (b) Percentage of late apoptosis (Annexin V with PI) after 1 and 3 days with different concentrations of delaminated MXene. (c) Percentage of necrosis (PI) after 1 or 3 days with different concentrations of delaminated MXene. The data are significant at $*p \leq 0.05$, $**p \leq 0.01$, $***p \leq 0.0001$, $****p \leq 0.0001$, $n = 6$ from three experiments. Two-way ANOVA was calculated by the GraphPad Prism 9 program.

and apoptosis. On the contrary, multilayered MXenes have a lower MXene-cell association, lower protein adsorption, and weaker other cellular effects leading to lower bioavailability than delaminated MXenes.

3. EXPERIMENTAL SECTION

3.1. Preparation of Delaminated MXenes

The delaminated Ti_3C_2Tx MXenes were synthesized by etching 0.5 g of the Ti_3AlC_2-based MAX phase in a 10 mL solution of 9 M hydrochloric acid (HCl) with dissolved 1.6 g of LiF. The synthesis beaker was thermostated for 24 h under constant mixing and washed by centrifugation to remove residual acids until a neutral pH was reached. The collected etching process products were mixed with 1 g of LiCl and stirred for an additional 18 h. Finally, the reaction mixture was centrifuged at 2550 *g* for 10 min, and the supernatant containing delaminated MXene was collected and concentrated to 5 g/L.

3.2. Preparation of Multilayered MXenes

Multilayered $Ti_3C_2T_x$ MXenes were synthesized by etching 0.2 g of the Ti_3AlC_2 MAX phase in 10 mL of concentrated HF. The suspension was stirred for 24 h at 35 °C. After this step, the suspension was centrifuged to remove the residual acids until the supernatant reached neutral pH. Finally, the MXenes were concentrated to 5 g/L.

3.3. Characterization of MXenes with SEM and XRD

Both the Ti_3AlC_2 MAX phase and the $Ti_3C_2T_x$ MXene morphology were investigated by scanning electron microscope (SEM) Helios NanoLab 650 from FEI (Eindhoven, The Netherlands). An X-ray powder diffractometer (XRD) from Rigaku (Tokyo, Japan) was applied for the phase composition determination.

3.4. Protein Corona Formation Analysis with ATR-FTIR

Delaminated or multilayered MXenes were incubated for 3 days in PBS, HUVEC medium, and HUVEC medium with 10% FBS to evaluate protein corona formation. After incubation, the passed samples were washed with PBS and centrifuged for 10 min at 16,000 *g* three times. ATR-FTIR measurements were performed using an Alpha spectrometer from Bruker Optik GmbH (Ettlingen, Germany) equipped with a single-reflection diamond ATR module and a deuterated triglycine sulfate (DTGS) detector. A total of 128 interferograms were acquired at a spectral resolution of 4 cm^{-1}, averaged, and Fourier-transformed into single-beam spectra using a Blackman–Harris three-term apodization function and a zero-filling factor of 2. Spectral preprocessing was carried out in OPUS software from Bruker Optik GmbH. The fingerprint region (400–1800 cm^{-1}) was extracted, atmospheric compensation applied, and baseline correction performed using the rubberband algorithm with 64 baseline points. To reduce high-frequency noise while preserving the band integrity, spectra were smoothed using a Savitzky–Golay filter with a 13-point window.

https://doi.org/10.1021/acsabm.6c01000
ACS Appl. Bio Mater. 2026, 9, 8158–8168

Downloaded from pubs.acs.org/aabmcb/article-pdf/9/17/8158/6651707/mt-2026-01000s.pdf by VILNIUS UNIV user on 04 November 2026

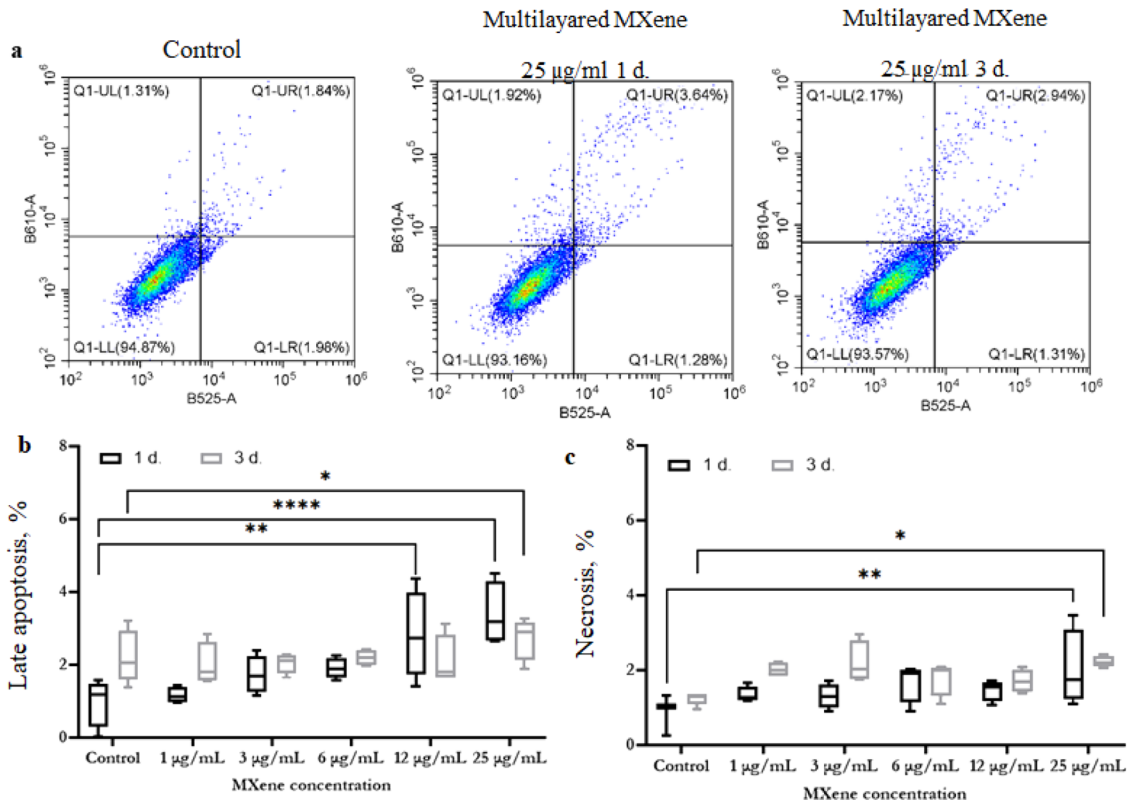


Figure 8. Percentage of late apoptosis (Annexin V with PI) and necrosis (PI) in HUVEC cells after 3 days of exposure to multilayered MXene. (a) HUVEC cell flowcharts—control cells, cells with 25 μg/mL multilayered MXene after 1 and 3 days of exposure. (b) Percentage of late apoptosis (Annexin V with PI) after 1 and 3 days with different concentrations of multilayered MXene. (c) Percentage of necrosis (PI) after 1 or 3 days with different concentrations of multilayered MXene. The data are significant at $*p \leq 0.05$, $**p \leq 0.01$, $***p \leq 0.0001$, $****p \leq 0.0001$, $n = 6$ from three experiments. Two-way ANOVA was calculated by GraphPad Prism 9 program.

3.5. Characterization of MXenes with Flow Cytometry

Optical properties of delaminated and multilayered MXenes were analyzed by flow cytometry. Violet, blue, and red laser side scatter was detected and compared to the water sample with an event rate lower than 200 events per second. Flow analysis was done by recording 1 min of events after event registration settled. Acquisition was done with CytoFLEX XL from Beckman Coulter (Brea, USA), and data analysis was performed with FCS express from De Novo Software (Los Angeles, USA).

3.6. Cultivation of Human Umbilical Vein Endothelial Cells (HUVECs)

HUVECs were obtained from Thermo Fisher Scientific (Waltham, USA) and cultivated in Human Large Vessel Endothelial Cell Basal Medium from Thermo Fisher Scientific (Waltham, USA) supplemented with 1× Large Vessel Endothelial Supplement from Thermo Fisher Scientific (Waltham, USA). For seeding experiments, cells were incubated in Trypsin-EDTA (0.05%) solution for 5 min at RT. Trypsin was inactivated by adding DMEM from Thermo Fisher Scientific (Waltham, USA) with 10% FBS from Thermo Fisher Scientific (Waltham, USA). Dislodged cells were centrifuged at 180*g* for 7 min and resuspended and cell count estimated with FastRead Slides with Counting Grid from Biosigma (Cona, Italy). Seeded cells were incubated with delaminated or multilayered MXene for 1 or 3 days.

3.7. Flow Cytometry Analysis of Delaminated and Multilayered MXene Association with HUVECs

HUVECs were seeded into six-well plates and allowed to adhere for 24 h. The following day, 1–25 μg/mL delaminated or multilayered MXene was added on the HUVECs and incubated for 1 or 3 days. During the day of the experiment, the cells were washed two to three times with PBS and lifted with Trypsin-EDTA, as described previously. To assess MXene-cell association, cells were analyzed using a CytoFLEX XL flow cytometer from Beckman Coulter (Brea, USA) with the red laser SSC-A detector.

3.8. HUVEC Viability after Exposure to Delaminated and Multilayered MXenes

HUVECs were seeded into a 96-well plate and allowed to adhere for 24 h. The following day, 1–25 μg/mL delaminated or multilayered MXene was added on the HUVECs and incubated for 1 or 3 days. During the day of the experiment, the HUVECs were washed twice with PBS and fixed with 4% PFA from Sigma-Aldrich (Burlington, USA) for 20 min at RT. After that, the cells were washed once with PBS and permeabilized with 0.1% Triton X-100 solution from Sigma-Aldrich (Burlington, USA) for 15 min at RT and washed once with PBS. The HUVECs were stained with 1 μg/mL DAPI from Thermo Fisher Scientific (Waltham, USA) solution for 5 min at RT. Stained nuclei pictures were taken with a fluorescence EVOS M7000 microscope from Thermo Fisher Scientific (Waltham, USA) and analyzed with Fiji for estimating cell count.

3.9. LDH Secretion after HUVEC Exposure to Delaminated and Multilayered MXenes

HUVECs were seeded into a 96-well plate and grown until 100% confluence was reached. 1 to 25 μg/mL delaminated or multilayered MXene was added on the HUVECs and incubated for 1 or 3 days. After incubation, the cultivation medium was collected and frozen for

Downloaded from pubs.acs.org/aabmcb/article-pdf/9/17/8158/6651707/mt-2026-01000s.pdf by VILNIUS UNIV user on 04 November 2026

https://doi.org/10.1021/acsabm.6c01000
ACS Appl. Bio Mater. 2026, 9, 8158−8168

evaluation of LDH release from cells. LDH activity was evaluated with Lactate Dehydrogenase Activity Assay Kit from Sigma-Aldrich (Burlington, USA) according to the manufacturer's recommendations. During the day of the measurement, the samples were thawed and centrifuged for 15 min at 3500 *g* for spun-down MXenes. LDH activity was detected at 450 nm by calculating substrate accumulation over times with a SpectraMax i3 (Molecular Devices, San Jose, USA) spectrophotometer.

3.10. HUVEC Apoptosis and Necrosis Following Exposure to Delaminated and Multilayered MXenes

HUVECs were seeded into a six-well plate and allowed to adhere for 24 h. The following day, 1–25 μg/mL delaminated or multilayered MXene was added on the HUVECs and incubated for 1 or 3 days. During the day of the experiment, the HUVECs were washed twice with PBS and lifted with trypsin according to the previously described procedure. Lifted cells were stained with Annexin V and PI kit (Abcam, Cambridge, UK) according to the manufacturer's recommendations. To measure apoptotic or necrotic cell percentage, cells were analyzed with a CytoFLEX XL flow cytometer from Beckman Coulter (Brea, USA). Cell samples were time-gated to include only periods during which instrument performance was stable. HUVEC cells were sequentially gated using a scatter gate (FSC-A vs SSC-A) to exclude debris, followed by a singlet gate (FSC-A vs FSC-H) to remove cell aggregates. Fluorescence quadrants were established using single-stained compensation controls. The alive (Annexin V and PI negative), early apoptotic (Annexin V positive and PI negative), late apoptotic (Annexin V and PI positive), and necrotic (Annexin V negative and PI positive) cells were identified.

3.11. Data Analysis and Statistics

Statistical analysis was done using GraphPad Prism 9.01 from GraphPad software (San Diego, USA). The data are expressed as means ± standard deviation (mean ± SD) based on three technical replicates from three independent experiments. Statistical significance was determined using two-way ANOVA, where $*p \leq 0.05$, $**p \leq 0.01$, $***p \leq 0.001$, $****p \leq 0.0001$.

4. CONCLUSIONS

In this study, we demonstrate that thin, flexible 2D sheets of $Ti_3C_2T_X$ MXene (1–2 nm in thickness and 5–10 μm in lateral dimension) generated stronger effects than multilayered MXenes with a 3D-like structure (2–5 μm in size). The size and structural differences between delaminated and multilayered MXenes were characterized by SEM and XRD and further supported by multiparametric, high-performance flow cytometry using side scatter parameters. Notably, the violet SSC-width parameter proved to be a useful tool for distinguishing differences in particle size and morphology.

Data showed that delaminated MXenes have a larger surface area, sharper and thinner 2D edges, and higher dispersibility and cellular contact than multilayered MXenes, which can be related to higher cell membrane damage and lower viability. These findings were confirmed by cytotoxicity assays (nuclei count and LDH release), showing stronger toxic effects of delaminated MXenes compared to multilayered MXenes. Furthermore, Annexin V/PI analysis also revealed that delaminated MXene more effectively induced late apoptosis and necrosis than multilayered ones.

Overall, the results suggest that the increased cytotoxicity of delaminated MXenes may be related to their morphological properties. Delaminated MXenes, due to their thin, sharp, and flexible 2D morphology, may interact more strongly with cellular membranes, potentially causing perturbation (by hypothetical "nano-knife" mechanism) with subsequent induction of cell membrane permeability causing viability changes and apoptosis that can be estimated by advanced, multiparametric, high-performance flow cytometry. In addition, the lower protein adsorption of delaminated MXenes, compared to multilayered MXenes, could also support their higher cytotoxicity. Thus, comparing MXenes with different sizes and morphological configurations provides valuable insight into structure–toxicity relationships and may help predict their biological effects.

■ ASSOCIATED CONTENT

Supporting Information

The Supporting Information is available free of charge at https://pubs.acs.org/doi/10.1021/acsabm.6c01000.

ROS measurement method description; ROS data after expose to MXene (DOCX)

■ AUTHOR INFORMATION

Corresponding Authors

Rokas Miksiunas – *Department of Regenerative Medicine, State Research Institute Centre for Innovative Medicine, Santariškių str. 5, LT-08406 Vilnius, Lithuania; Laboratory of Nanotechnology, Center for Physical Sciences and Technology, Sauletekio Ave. 3, LT-10257 Vilnius, Lithuania;* Email: rokas.miksiunas@ftmc.lt

Arunas Ramanavicius – *Laboratory of Nanotechnology, Center for Physical Sciences and Technology, Sauletekio Ave. 3, LT-10257 Vilnius, Lithuania; Department of Physical Chemistry, Faculty of Chemistry, Vilnius University, Sauletekio Av. 3, LT-10257 Vilnius, Lithuania;* orcid.org/0000-0002-0885-3556; Email: arunas.ramanavicius@chf.vu.lt

Authors

Rusne Uzielaite – *Department of Regenerative Medicine, State Research Institute Centre for Innovative Medicine, Santariškių str. 5, LT-08406 Vilnius, Lithuania*

Simonas Ramanavicius – *Department of Electrochemical Material Science, Centre for Physical Sciences and Technology, Sauletekio Ave. 3, LT-10257 Vilnius, Lithuania;* orcid.org/0000-0003-1432-3866

Sonata Adomaviciute-Grabusove – *Department of Physical Chemistry, Faculty of Chemistry, Vilnius University, Sauletekio Av. 3, LT-10257 Vilnius, Lithuania*

Sigita Bendinskaite – *Department of Physical Chemistry, Faculty of Chemistry, Vilnius University, Sauletekio Av. 3, LT-10257 Vilnius, Lithuania*

Kieran Brennan – *Conway Institute of Biomolecular and Biomedical Research, University College Dublin (UCD), 8Q6G+33 Dublin 4, Ireland*

Alfonso Blanco – *Flow Cytometry Core Technology, UCD Conway Institute of Biomolecular and Biomedical Research, University College Dublin (UCD), 8Q6G+33 Dublin 4, Ireland*

Maksym Pogorielov – *Biomedical Research Centre, Medical Institute, Sumy State University, 116, Kharkivska, 40007 Sumy, Ukraine; Institute of Atomic Physics and Spectroscopy, University of Latvia, Jelgavas iela 3, LV-1004 Riga, Latvia;* orcid.org/0000-0001-9372-7791

Downloaded from pubs.acs.org/aabmcb/article-pdf/9/17/8158/6651570/mt-2026-01000s.pdf by VILNIUS UNIV user on 04 November 2026

https://doi.org/10.1021/acsabm.6c01000
ACS Appl. Bio Mater. 2026, 9, 8158–8168

Viktoriia Korniienko – *Biomedical Research Centre, Medical Institute, Sumy State University, 116, Kharkivska, 40007 Sumy, Ukraine; Institute of Atomic Physics and Spectroscopy, University of Latvia, Jelgavas iela 3, LV-1004 Riga, Latvia*

Daiva Bironaite – *Department of Regenerative Medicine, State Research Institute Centre for Innovative Medicine, Santariškių str. 5, LT-08406 Vilnius, Lithuania*

Oleksiy Gogotsi – *Materials Research Center, Ltd., Materials Research Center, Ltd., Krzhyzhanovskogo str. 3,03142 Kyiv, Ukraine; A.J. Drexel Nanomaterials Institute and Materials Science & Engineering Department, Drexel University, 3141 Chestnut Street, Philadelphia, Pennsylvania 19104, United States*

Complete contact information is available at: https://pubs.acs.org/doi/10.1021/acsabm.6c01000

Author Contributions

The manuscript was written through contributions of all authors. All authors have given approval to the final version of the manuscript.

Notes

The authors declare no competing financial interest.

■ ACKNOWLEDGMENTS

This work was supported by the Research Council of Lithuania (LMTLT), agreement no. S-PD-24-41.

■ ABBREVIATIONS

ANOVA	analysis of variance
DAPI	4′,6-diamidino-2-phenylindole
DMEM	Dulbecco's Modified Eagle Medium
EDTA	ethylenediaminetetraacetic acid
FBS	fetal bovine serum
HCl	hydrochloric acid
HF	hydrofluoric acid
HUVEC	human umbilical vein endothelial cells
LDH	lactate dehydrogenase
LiCl	lithium chloride
LiF	lithium fluoride
LVES	large vessel endothelial supplement
MAX	Mn+1AXn layered precursor phase (e.g., Ti_3AlC_2)
MFI	mean fluorescence intensity
MXene	two-dimensional transition metal carbides and nitrides
PBS	phosphate-buffered saline
PFA	paraformaldehyde
PI	propidium iodide
ROS	reactive oxygen species
RT	room temperature
SSC	side scatter
XRD	X-ray diffraction

■ REFERENCES

(1) Ho, P. Twenty Years of 2D Materials. *Nat. Phys.* **2024**, *20* (1), No. 1.

(2) Dhamodharan, D.; Al-Harthi, M. A.; Ramya, B.; Bafaqeer, A.; Alam, F. MXenes: A Promising Material with Multifunctional Applications. *J. Environ. Chem. Eng.* **2024**, *12* (2), No. 112316.

(3) Ulas, B.; Çetin, T.; Kaya, Ş.; Akinay, Y.; Kivrak, H. Novel $Ti_3C_2X_2$ MXene Supported $BaMnO_3$ Nanoparticles as Hydrazine Electrooxidation Catalysts. *Int. J. Hydrogen Energy* **2024**, *58*, 726–736.

(4) Karataş, Y.; Çetin, T.; Akinay, Y.; Gülcan, M. Synthesis and Characterization of Pd Doped MXene for Hydrogen Production from the Hydrolysis of Methylamine Borane: Effect of Cryogenic Treatment. *J. Energy Inst.* **2023**, *109*, No. 101310.

(5) Saleth, L. R.; Gupta, M.; Sharma, G.; Verma, E.; Dhingra, S. Meta-Analyses of the Evolution of MXene Synthesis for Bioengineering and Artificial Intelligence-Driven Applications. *Commun. Mater.* **2025**, *6* (1), No. 289.

(6) Baghchesaraee, K.; Ghasali, E.; Raza, S.; Babenko, A.; Paimard, G.; Bashir, T.; Maleki-Ghaleh, H.; Jie, L.; Orooji, Y. Recent Advancements in MXenes Synthesis, Properties, and Cutting-Edge Applications: A Comprehensive Review. *J. Environ. Chem. Eng.* **2024**, *12* (5), No. 113546.

(7) Mahmud, S. T.; Hasan, M. M.; Bain, S.; Rahman, S. T.; Rhaman, M.; Hossain, M. M.; Ordu, M. Multilayer MXene Heterostructures and Nanohybrids for Multifunctional Applications: A Review. *ACS Materials Lett.* **2022**, *4* (6), 1174–1206.

(8) Phan, T. N. L.; Nguyen, T. X.; Truong, T. T.; Duong, T. K. N.; Doan, V. H. M.; Vo, T. T.; Misra, M.; Choi, J.; Pal, U.; Oh, J.; Mondal, S. Advancements, Challenges, and Future Perspectives of MXenes in Biomedicine. *SmartMat* **2025**, *6* (2), No. e70009.

(9) Zhang, J.; Fu, Y.; Mo, A. Multilayered Titanium Carbide MXene Film for Guided Bone Regeneration. *Int. J. Nanomed.* **2019**, *14*, 10091–10103.

(10) Karatas, E.; Topuz, M.; Akinay, Y. Ti_2 NT_x MXene and Carbon Quantum Dots Modified Chitosan Scaffold for Potential Wound Healing: In Vitro Assessment of Cytotoxicity, Hemocompatibility, Antioxidant, and Antibacterial Properties. *Small Methods* **2025**, *9* (12), No. e01415.

(11) Ramezani Farani, M.; Mirzaee, D.; Hatami, A.; Kumar, K.; Ghoreishian, S. M.; Huh, Y. S. Biocompatibility and Immunomodulation of MXenes for Targeted Delivery of Bioactive Agents and Drugs. *Bioact. Mater.* **2026**, *55*, 546–567.

(12) Akinay, Y.; Karatas, E.; Ruzgar, D.; Akbari, A.; Baskin, D.; Cetin, T.; Kazici, H. C.; Topuz, M. Cytotoxicity and Antibacterial Activity of Polyhedral Oligomeric Silsesquioxane Modified $Ti_3C_2T_x$ MXene Films. *Sci. Rep.* **2025**, *15* (1), No. 8463.

(13) Arabi Shamsabadi, A.; Sharifian Gh, M.; Anasori, B.; Soroush, M. Antimicrobial Mode-of-Action of Colloidal $Ti_3C_2T_x$ MXene Nanosheets. *ACS Sustainable Chem. Eng.* **2018**, *6* (12), 16586–16596.

(14) Kyrylenko, S.; Chorna, I.; Klishchova, Z.; Yanko, I.; Roshchupkin, A.; Deineka, V.; Diedkova, K.; Konieva, A.; Petrichenko, O.; Kube-Golovin, I.; Wennemuth, G.; Coy, E.; Roslyk, I.; Baginskiy, I.; Zahorodna, V.; Gogotsi, O.; Chacon, B.; Cartarozzi, L. P.; Oliveira, A. L. R.; Iatsunskyi, I.; Gogotsi, Y.; Pogorielov, M. Elucidation of Potential Genotoxicity of MXenes Using a DNA Comet Assay. *ACS Appl. Bio Mater.* **2024**, *7* (12), 8351–8366.

(15) Ganguly, P.; Breen, A.; Pillai, S. C. Toxicity of Nanomaterials: Exposure, Pathways, Assessment, and Recent Advances. *ACS Biomater. Sci. Eng.* **2018**, *4* (7), 2237–2275.

(16) Behzadi, S.; Serpooshan, V.; Tao, W.; Hamaly, M. A.; Alkawareek, M. Y.; Dreaden, E. C.; Brown, D.; Alkilany, A. M.; Farokhzad, O. C.; Mahmoudi, M. Cellular Uptake of Nanoparticles: Journey inside the Cell. *Chem. Soc. Rev.* **2017**, *46* (14), 4218–4244.

(17) Li, Y.; Yuan, H.; Von Dem Bussche, A.; Creighton, M.; Hurt, R. H.; Kane, A. B.; Gao, H. Graphene Microsheets Enter Cells through Spontaneous Membrane Penetration at Edge Asperities and Corner Sites. *Proc. Natl. Acad. Sci. U. S. A.* **2013**, *110* (30), 12295–12300.

(18) Kettler, K.; Veltman, K.; Van De Meent, D.; Van Wezel, A.; Hendriks, A. J. Cellular Uptake of Nanoparticles as Determined by Particle Properties, Experimental Conditions, and Cell Type. *Environ. Toxicol. Chem.* **2013**, *33* (3), 481–492.

(19) Shurbaji, S.; Manaph, N. P. A.; Ltaief, S. M.; Al-Shammari, A. R.; Elzatahry, A.; Yalcin, H. C. Characterization of MXene as a Cancer Photothermal Agent Under Physiological Conditions. *Front. Nanotechnol.* **2021**, *3*, No. 689718.

Downloaded from pubs.acs.org/aabmcb/article-pdf/9/17/8158/6651707/mt-2026-01000s.pdf by VILNIUS UNIV user on 04 November 2026

(20) Wu, W.; Ge, H.; Zhang, L.; Lei, X.; Yang, Y.; Fu, Y.; Feng, H. Evaluating the Cytotoxicity of Ti_3C_2 MXene to Neural Stem Cells. *Chem. Res. Toxicol.* **2020**, *33* (12), 2953–2962.
(21) Adomaviciute-Grabusove, S.; Popov, A.; Ramanavicius, S.; Sablinskas, V.; Shevchuk, K.; Gogotsi, O.; Baginskiy, I.; Gogotsi, Y.; Ramanavicius, A. Monitoring $Ti_3C_2T_x$ MXene Degradation Pathways Using Raman Spectroscopy. *ACS Nano* **2024**, *18* (20), 13184–13195.
(22) Ghotia, S.; Kumar, A.; Sudarsan, V.; Dwivedi, N.; Singh, S.; Kumar, P. Multilayered $Ti_3C_2T_x$ MXenes: A Prominent Materials for Hydraogen Storage. *Int. J. Hydrogen Energy* **2024**, *52*, 100–107.
(23) Breznica, P.; Koliqi, R.; Daka, A. A Review of the Current Understanding of Nanoparticles Protein Corona Composition. *Med. Pharm. Rep.* **2020**, *93* (4), 342–350.
(24) Sadat, A.; Joye, I. J. Peak Fitting Applied to Fourier Transform Infrared and Raman Spectroscopic Analysis of Proteins. *Appl. Sci.* **2020**, *10* (17), No. 5918.
(25) Cheng, X.; Tian, X.; Wu, A.; Li, J.; Tian, J.; Chong, Y.; Chai, Z.; Zhao, Y.; Chen, C.; Ge, C. Protein Corona Influences Cellular Uptake of Gold Nanoparticles by Phagocytic and Nonphagocytic Cells in a Size-Dependent Manner. *ACS Appl. Mater. Interfaces* **2015**, *7* (37), 20568–20575.
(26) Magesh, V.; Atchudan, R.; Arya, S.; Mahadevegowda, S. H.; Sundramoorthy, A. K. Tailored Synthesis and Morphological Analysis of Mo_2CT_x and $Ti_3C_2T_x$ MXenes: A Study on Multilayered and Delaminated Architectures. *Nanoscale Adv.* **2025**, *7* (24), 8122–8137.
(27) Agagliate, J.; Röttgers, R.; Twardowski, M. S.; McKee, D. Evaluation of a Flow Cytometry Method to Determine Size and Real Refractive Index Distributions in Natural Marine Particle Populations. *Appl. Opt.* **2018**, *57* (7), No. 1705.
(28) Woud, W. W.; Pugsley, H. R.; Bettin, B. A.; Varga, Z.; Van Der Pol, E. Size and Fluorescence Calibrated Imaging Flow Cytometry: From Arbitrary to Standard Units. *Cytometry, Part A* **2024**, *105* (10), 752–762.
(29) Zhang, W.; Tian, Y.; Hu, X.; He, S.; Niu, Q.; Chen, C.; Zhu, S.; Yan, X. Light-Scattering Sizing of Single Submicron Particles by High-Sensitivity Flow Cytometry. *Anal. Chem.* **2018**, *90* (21), 12768–12775.
(30) Tonkaboni, A.; Tatar, A.; Motlagh, K. H.; Fekrazad, R. The Cytotoxic Effect of 4 Different Wavelengths of Low-Level Laser Therapy on Squamous Cell Carcinoma – An Invitro Study. *J. Craniomaxillofac. Res.* **2024**, *11* (1), 26–34.
(31) Diedkova, K.; Roslyk, I.; Kanas, N.; Grine, L.; Deineka, V.; Blacha-Grzechnik, A.; Boroduskis, M.; Iatsunskyi, I.; Anastaziak, B.; Konieva, A.; Shubin, P.; Simka, W.; Truhins, M.; Sulaieva, O.; Yanko, I.; Zahorodna, V.; Stojanovic, G.; Gogotsi, O.; Gogotsi, Y.; Pogorielov, M. Effects of Etching and Delamination on Biocompatibility of Ti-Based MXenes. *ACS Appl. Mater. Interfaces* **2025**, *17* (34), 47919–47937.
(32) Dong, T.; Qi, M.; Ji, S.; Liu, K.; Shi, P.; Geng, C. Effect of Ti_3C_2-MXene Size on Cell Viability of Human Carcinoma Cells. *Micromater. Interfaces* **2024**, *2* (1), No. 6307.
(33) Wu, J.; Yu, Y.; Su, G. Safety Assessment of 2D MXenes: In Vitro and In Vivo. *Nanomaterials* **2022**, *12* (5), No. 828.
(34) Rashid, B.; Anwar, A.; Shahabuddin, S.; Mohan, G.; Saidur, R.; Aslfattahi, N.; Sridewi, N. A Comparative Study of Cytotoxicity of PPG and PEG Surface-Modified 2-D Ti_3C_2 MXene Flakes on Human Cancer Cells and Their Photothermal Response. *Materials* **2021**, *14* (16), No. 4370.
(35) Bala, K.; Ambwani, K.; Gohil, N. K. Effect of Different Mitogens and Serum Concentration on HUVEC Morphology and Characteristics: Implication on Use of Higher Passage Cells. *Tissue Cell* **2011**, *43* (4), 216–222.
(36) Li, T.; Ma, J.; Wang, W.; Lei, B. Bioactive MXene Promoting Angiogenesis and Skeletal Muscle Regeneration through Regulating M2 Polarization and Oxidation Stress. *Adv. Healthcare Mater.* **2023**, *12* (4), No. 2201862.
(37) Zhang, D.; Zheng, W.; Li, X.; Li, A.; Ye, N.; Zhang, L.; Liu, Y.; Liu, X.; Zhang, R.; Wang, M.; Cheng, J.; Yang, H.; Gong, M. Investigating the Effect of Ti_3C_2 (MXene) Nanosheet on Human Umbilical Vein Endothelial Cells via a Combined Untargeted and Targeted Metabolomics Approach. *Carbon* **2021**, *178*, 810–821.
(38) Lesniak, A.; Fenaroli, F.; Monopoli, M. P.; Åberg, C.; Dawson, K. A.; Salvati, A. Effects of the Presence or Absence of a Protein Corona on Silica Nanoparticle Uptake and Impact on Cells. *ACS Nano* **2012**, *6* (7), 5845–5857.
(39) Marchwiany, M. E.; Birowska, M.; Popielski, M.; Majewski, J. A.; Jastrzębska, A. M. Surface-Related Features Responsible for Cytotoxic Behavior of MXenes Layered Materials Predicted with Machine Learning Approach. *Materials* **2020**, *13* (14), No. 3083.
(40) Scheibe, B.; Wychowaniec, J. K.; Scheibe, M.; Peplińska, B.; Jarek, M.; Nowaczyk, G.; Przysiecka, Ł. Cytotoxicity Assessment of Ti–Al–C Based MAX Phases and $Ti_3C_2T_x$ MXenes on Human Fibroblasts and Cervical Cancer Cells. *ACS Biomater. Sci. Eng.* **2019**, *5* (12), 6557–6569.
(41) Dmytriv, T. R.; Lushchak, V. I. Potential Biosafety of Mxenes: Stability, Biodegradability, Toxicity and Biocompatibility. *Chem. Rec.* **2024**, *24* (4), No. e202300338.
(42) Rahman, U. U.; Humayun, M.; Ghani, U.; Usman, M.; Ullah, H.; Khan, A.; El-Metwaly, N. M.; Khan, A. MXenes as Emerging Materials: Synthesis, Properties, and Applications. *Molecules* **2022**, *27* (15), No. 4909.

Downloaded from pubs.acs.org/aabmcb/article-pdf/9/17/8158/6651507/mt-2026-01000s.pdf by VILNIUS UNIV user on 04 November 2026

https://doi.org/10.1021/acsabm.6c01000
ACS Appl. Bio Mater. 2026, 9, 8158–8168